



# Reducing Acquisition Time of Diffusion Weighted MR Imaging of the Rectum with Simultaneous Multi-Slice Acquisition: A Reader Study

Tijmen Koëter, MD, Germaine Jongen, PhD, Eline Hanrath-Vos, PhD, Ewoud Smit, PhD, Jurgen Fütterer, PhD, Marnix Maas, PhD, Tom Scheenen, PhD

**Rationale and Objectives:** To assess the acquisition time and image quality of simultaneous multislice-accelerated diffusion-weighted imaging (SMS-DWI) versus conventional DWI (C-DWI) of the rectum.

**Materials and Methods:** In patients scheduled for a magnetic resonance imaging of the rectum, both SMS-DWI and C-DWI were performed on a 3T whole body magnetic resonance scanner. Image quality of the DWI sequences was reviewed by two independent radiologists who were blinded to the method of imaging using a five-point Likert scale: (score ranging from 1 (non-diagnostic) to 5 (excellent)). The mean scores of SMS-DWI versus C-DWI were compared for the individual readers using a nonparametric test (Wilcoxon signed ranks).

**Results:** The SMS-DWI protocol acquisition time was 4:08 min vs. 7:24 min per patient, which led to a reduction of 44.1% for the C-DWI protocol, both excluding time for sequence specific adjustments (shimming). No statistical differences between the conventional-, and SMS- diffusion weighted images were seen for both readers. Mean overall image quality of the SMS-DWI TRACE images was 3.5 (SD: 1.3) and 3.3 (SD: 1.0) for reader 1 and reader 2, respectively. Mean overall image quality of the C-DWI TRACE images was 3.4 (SD: 1.3) and 3.2 (SD: 1.1) for reader 1 and reader 2, respectively.

**Conclusion:** Optimized SMS-DWI compared to C-DWI in imaging of the rectum showed similar image quality while a significant acquisition time reduction was achieved.

**Key Words:** Rectal cancer staging; Neoadjuvant chemoradiotherapy; Simultaneous multi-slice acquisition; Diffusion weighted imaging.

© 2022 The Association of University Radiologists. Published by Elsevier Inc. This is an open access article under the CC BY license (<http://creativecommons.org/licenses/by/4.0/>)

## INTRODUCTION

In current clinical practice, magnetic resonance imaging (MRI) is used for tumor staging and follow up of rectal cancer. According to the consensus guidelines of the European Society of Gastrointestinal and Abdominal

Radiology, MRI is the method of choice for primary staging as well as restaging of rectal cancer (1). The added value of diffusion weighted imaging (DWI) in combination with conventional T2-weighted imaging in the detection, especially after neoadjuvant (chemo)radiotherapy (CRT), of rectal cancer has also been shown in several studies (2–4). As a result, DWI was added to the European Society of Gastrointestinal and Abdominal Radiology guidelines, which state that a routine rectum MRI examination protocol should at least consist of T2-weighted imaging and diffusion-weighted imaging including a  $b$ -value of minimal  $800 \text{ s/mm}^2$ . After staging based on MRI and endoscopy, treatment generally consists of radical surgery with or without neoadjuvant CRT, depending on tumor and nodal stage. Currently however, a paradigm shift is ongoing towards organ preservation in rectal cancer treatment (5). A complete response (no residual tumor) to neoadjuvant CRT treatment is observed in 10–30% of patients in whom active surveillance (watch-and-

### Acad Radiol 2022; 29:1802–1807

From the Department of Medical Imaging, Radboud University Medical Center, Geert Grooteplein Zuid 10, Nijmegen, The Netherlands (T.K., E.S., J.F., M.M., T.S.); Department of Surgery, Radboud University Medical Center, Geert Grooteplein Zuid 10, Nijmegen, The Netherlands (T.K.); Department of Radiation Oncology, Radboud University Medical Center, Nijmegen, The Netherlands (G.J.); Department of Radiology, Elisabeth-TweeSteden Ziekenhuis (ETZ), Tilburg, The Netherlands (E.H.-V.). Received December 16, 2021; revised February 3, 2022; accepted February 5, 2022. **Address correspondence to:** Tijmen Koëter, MD Radboudumc, Department of Medical Imaging, Geert Grooteplein Zuid 10, 6525GA Nijmegen, The Netherlands e-mail: [tijmen.koeter@radboudumc.nl](mailto:tijmen.koeter@radboudumc.nl)

© 2022 The Association of University Radiologists. Published by Elsevier Inc. This is an open access article under the CC BY license (<http://creativecommons.org/licenses/by/4.0/>) <https://doi.org/10.1016/j.acra.2022.02.005>

wait) may be a viable option (6–8). This has led to an increase of patients who are participating in an international watch-and-wait surveillance registry, in which 3-monthly repeated MR examinations including DWI have an important role (9).

Although DWI is advised as an essential part of an MRI examination protocol of the rectum, its clinical application suffers from relatively long acquisition times caused by the large number of slices needed to cover the entire rectum and the multiple  $b$ -values and diffusion directions used in these acquisitions. Faster imaging methods are therefore warranted. A first and commonly used step to reduce acquisition times is to use parallel imaging techniques, such as SENSE or generalized autocalibrating partial parallel acquisition. These techniques come at the cost of loss of signal to noise (SNR) because of less time spent on the total acquisition and because of so-called  $g$ -factor noise in areas where there is little difference in coil sensitivity from the different elements of the used coil array,

An acceleration technique that is currently emerging is known as simultaneous multi-slice (SMS) (10). With this technique, the signal of multiple simultaneously excited slices can be disentangled based on the individual signals of multiple coil elements. Acquiring multiple slices simultaneously has the potential to reduce acquisition time without accompanying SNR loss (only some  $g$ -factor noise could remain), thereby increasing patient comfort and improving clinical use of DWI. Exciting and refocusing multiple slices at once also reduces overall radiofrequency power deposition.

The choice of fat suppression method can have a strong impact on scanning time. Although the spectral adiabatic inversion recovery (SPAIR) method is commonly used in large field of view (FOV) rectal DWI, the inversion delay it requires causes a significant increase in acquisition time, and the adiabatic inversion pulse requires a substantial amount of radiofrequency power. The SMS technique allows to use the SPAIR technique over a large FOV with many slices within a reasonable acquisition time. With conventional multi-slice DWI, chemical shift selective fat suppression avoids the use of long inversion delays, at the cost of an increased sensitivity to B1 inhomogeneity, which may lead to incomplete fat suppression at the edges of a large FOV. In practice this can be mitigated by acquiring multiple image volumes at multiple table positions, at the cost of the extra time for multiple acquisitions, additional table movement with associated transmitter and coil adjustments and additional shimming.

Simultaneous multislice-accelerated DWI (SMS-DWI) has proven success in various body parts, such as the prostate, kidney, liver, and pancreas (11–14). More recently, Park et al were the first to report on the feasibility of SMS-DWI in MRI of the rectum and described a substantial reduction in acquisition time while maintaining image quality (15). They however, used endorectal filling of the rectum which is not recommended in the latest European guidelines (1,16). With differences in body composition between Asians and European population (body mass index and body-fat percent) (17), validation of SMS DWI vs. conventional DWI with

spectral fat saturation in European patients without endorectal filling is still a gap in current literature.

Therefore, the aim of this study is to compare the currently used optimized conventional DWI pulse sequence with chemical shift selective fat saturation vs. the recently developed SMS-DWI pulse sequence with SPAIR fat suppression in patients undergoing an MRI examination of the rectum, with respect to acquisition time and image quality.

## METHODS

### Patient Population

Patients who were scheduled for an MRI of the rectum between June 2018 and October 2019 for rectal cancer (re) staging or follow-up were asked to participate in the study. The study was approved by the institutional ethics review board and all patients signed informed consent.

### MR Imaging Protocol

MR images were obtained on a whole-body 3 T MR scanner (Siemens Magnetom<sup>®</sup> Prisma-Fit, Erlangen, Germany) using a spine and body phased array coil. Patients received laxative (Dulcolax or Microlax) followed by a bowel movement and antispasmodic medication (Buscopan) (1 hour and 5–10 minutes, respectively) prior to the MRI examination and were placed on the MR table in supine, feet first position. After scout scanning, the conventional protocol started with a three-dimensional T1-weighted starvibe sequence and T2-weighted TSE scans in sagittal, coronal and transversal directions. After these anatomical scans, DWI data were acquired with the conventional DWI pulse sequence, consisting of two stacks of multi-slice spin echo echo-planar imaging (se-EPI) scans with 35 slices each, at two slightly overlapping table positions. With a repetition time (TR) of 4.4 seconds this pulse sequence took 7:24 minutes excluding adjustments. Immediately after these, a single large FOV SMS-DWI EPI protocol covering the same area was used to acquire 70 slices (two simultaneous slices) at one table position with TR of 4.6 seconds and total acquisition time of 4:08 minutes. Parameters of the SMS-DWI sequence defining spatial resolution and diffusion weighting were set to meet the conventional DWI settings as closely as possible (Table 1). Other parameters were chosen as short and optimal as possible for both pulse sequences for optimized performance of each. Diffusion weighted images were obtained for three  $b$ -values (50, 400, and 800 s/mm<sup>2</sup> with 1, 6, and 8 averages, respectively) in three orthogonal directions, from which a trace-weighted image was calculated. Furthermore, a calculated  $b$ -value of 1000 s/mm<sup>2</sup> was reconstructed and ADC maps were created. All scans were acquired in free breathing.

### Image Analysis

A qualitative image analysis was independently performed by two radiologists who were blinded to the method of imaging

**TABLE 1. Overview of the MRI Settings of Both Scanning Protocols**

| MRI Protocol  | DWI se-EPI                      | SMS DWI EPI  |
|---|---------------------------------|--|
| Orientation   | Transversal                     | Transversal  |
| TR/TE (ms)  | 4400/63                         | 4600/52  |
| FOV (mm)  | 276×276                         | 276×276  |
| Voxel size (mm)   | 2.2×2.2×3.0                     | 2.2×2.2×3.0  |
| Number of slices  | 2 slice groups of 35            | 70   |
| <i>b</i> -value (calc <i>b</i> -value) (s/mm <sup>2</sup> ) | 50, 400, 800, (1000)            | 50, 400, 800, (1000)                                     |
| averages  | 1, 6, 8                         | 1, 6, 8  |
| Diffusion mode  | Monopolar, 3-scan trace         | Monopolar, 3-scan trace                                  |
| Echo spacing (ms)   | 0,65                            | 0.55   |
| Bandwidth (Hz/Px)   | 1776                            | 2170   |
| Fat suppression   | CHESS                           | SPAIR  |
| Acceleration factor   | Partial Fourier 6/8<br>GRAPPA 2 | Partial Fourier 7/8<br>GRAPPA 2<br>2 simultaneous slices |
| Acquisition time  | 7:24 min (2×3:42 min)           | 4:08 min   |

CHESS, chemical shift selective; DWI, diffusion weighted imaging; EPI, echo planar imaging; FOV, field of view; GRAPPA, generalized autocalibrating partial parallel acquisition; SMS, simultaneous multislice; SPAIR, spectrally adiabatic inversion recovery; TE, echo time; TR, repetition time.

(with 12 and 9 years of experience in reading abdominal MRI). On the TRACE-weighted images (geometric mean diffusion weighted image of three orthogonal diffusion directions), the calculated *b*-value (*b*-1000) and calculated ADC images, the following criteria were rated on a five-point Likert scale: image quality of the mesorectum, subcutaneous and overall image quality (1: non-diagnostic; 2: poor; 3: satisfactory; 4: good; 5: excellent), quality of fat suppression and

visibility of structures (rectum, lymph nodes, tumor, vasculature, bone, prostate) (0: structure not present at T1/T2; 1: poor; 2: fair; 3: good; 4: very good; 5: excellent; 6: not applicable) and the presence of artifacts (1: non-diagnostic; 2: substantial; 3: moderate; 4: minor; 5: absent). Conventional DWI and SMS DWI sequences were individually presented to the radiologists in random order in a home-built workstation implemented in MevisLab (MeVis Medical Solutions AG, Bremen, Germany).

**Statistical Analysis**

After scoring of the images, results were imported in GraphPad (GraphPad Prism, San Diego, California, USA), SPSS (IBM, Armonk, New York, USA) and R (R Foundation for Statistical Computing, Vienna, Austria) for statistical analysis. The mean score of each criterion described above was calculated for the conventional and SMS images per individual reader. The scores were compared using nonparametric tests (Wilcoxon Signed Ranks). Differences were considered statistically significant at *p* < 0.05. Interobserver agreement of image quality was analyzed by calculating the weighted kappa coefficient. Kappa values of <0.00 show poor, 0.00–0.20 slight, 0.21–0.40 fair, 0.41–0.60 moderate, 0.61–0.80 substantial and 0.81–1.00 almost perfect agreement (18).

**RESULTS**

In total, 27 patients (21 male:6 female) were included in the study, median age was 64 years old (range 35–77). Data were acquired for all patients successfully and no data sets had to be excluded Figure 1. shows examples of image acquisitions.

Per patient, conventional DWI protocol acquisition time was 7:24 minutes vs. 4:08 minutes for the SMS-DWI protocol, excluding time for table movement and sequence specific adjustments (shimming).

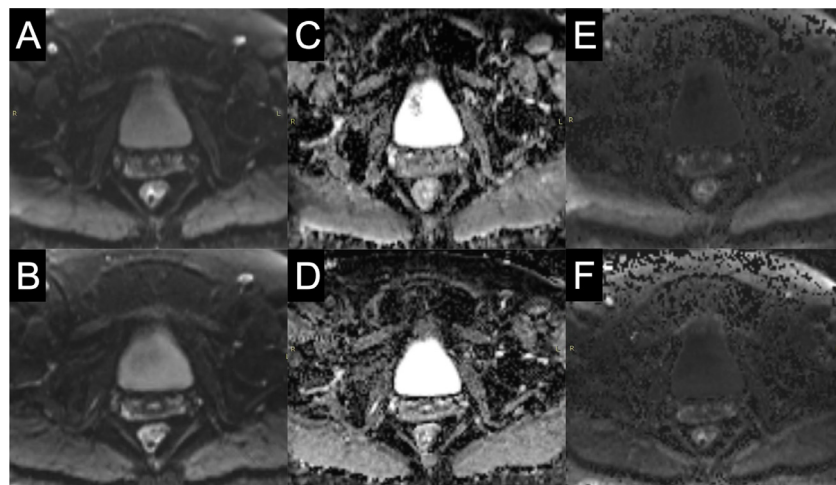


**Figure 1.** Axials views of the pelvis of a female patient, 74 years old. The upper row of images are conventional se-EPI diffusion weighted images, below the corresponding SMS-DWI images. (a, b) shows the TRACE images, (c, d) calculated *b*-value (B1000) images and (e, f) the calculated ADC images. EPI, echo planar imaging; SMS-DWI, simultaneous multislice-accelerated diffusion-weighted imaging.

TABLE 2. Summary of Scores (Mean, SD) of Image Quality Parameters by the Individual Readers for Conventional-, and SMS-DWI

|  | Reader 1     |             |         | Reader 2     |             |         |
|--|--------------|-------------|---------|--------------|-------------|---------|
|  | Conventional | SMS         | p Value | Conventional | SMS         | p Value |
| <b>Overall image quality*</b>                                      |              |             |         |              |             |         |
| TRACE  | 3.41 (1.31)  | 3.51 (1.25) | 0.82    | 3.19 (1.08)  | 3.30 (1.03) | 0.53    |
| Calculated B-value (B1000)   | 2.41 (1.01)  | 2.22 (1.09) | 0.49    | 2.93(1.02)   | 3.11 (1.01) | 0.25    |
| ADC  | 1.93 (0.96)  | 1.74 (0.76) | 0.39    | 2.81 (1.14)  | 2.85 (1.06) | 0.82    |
| Quality of fat suppression mesorectum (TRACE)*                     | 3.56 (1.34)  | 3.59 (1.28) | 0.95    | 3.26 (1.02)  | 3.22 (1.01) | 0.86    |
| <b>Visibility of rectum#</b>                                       |              |             |         |              |             |         |
| TRACE  | 3.52 (1.41)  | 3.58 (1.33) | 0.92    | 3.29 (1.12)  | 3.26 (0.96) | 0.87    |
| Calculated B-value (B1000)   | 3.24 (1.36)  | 3.27 (1.22) | 0.90    | 3.00 (1.02)  | 3.09 (1.00) | 0.71    |
| ADC  | 2.60 (1.19)  | 2.61 (0.98) | 0.81    | 3.00 (1.06)  | 2.96 (0.88) | 0.81    |
| <b>Visibility of lymph nodes#</b>                                  |              |             |         |              |             |         |
| TRACE  | 3.07 (1.27)  | 3.15 (1.20) | 0.80    | 2.44 (0.70)  | 2.44 (0.80) | 1.00    |
| Calculated B-value (B1000)   | 1.59 (0.69)  | 1.93 (0.92) | 0.11    | 1.62 (0.56)  | 1.67 (0.62) | 0.80    |
| ADC  | 1.19 (0.40)  | 1.33 (0.48) | 0.21    | 1.03 (0.19)  | 1.08 (0.27) | 0.56    |
| Air/susceptibility differences in mesorectum in TRACE <sup>§</sup> | 3.15 (1.46)  | 3.33 (1.24) | 0.68    | 4.07 (1.04)  | 3.93 (0.96) | 0.62    |
| Motion artifact in ADC <sup>§</sup>                                | 2.65 (1.27)  | 2.70 (0.91) | 0.76    | 4.67 (0.83)  | 4.85 (0.53) | 0.26    |

DWI, diffusion weighted imaging; SMS, simultaneous multi-slice.

\* 1: non-diagnostic; 2: poor; 3: satisfactory; 4: good; 5: excellent.

# 0: structure not present at T1/T2; 1: poor; 2: fair; 3: good; 4: very good; 5: excellent; 6: not applicable.

§ 1: non-diagnostic; 2: substantial; 3: moderate; 4: minor; 5: absent.

## Qualitative Assessment

A summary of the scores of image quality parameters of both readers is shown in Table 2. Average image quality scores were similar for the conventional and SMS technique for parameters without statistical difference for both readers. Mean overall image quality of the SMS-DWI TRACE images (score ranging from 1 (non-diagnostic) to 5 (excellent)) was 3.5 (SD: 1.3) and 3.3 (SD: 1.0) for reader 1 and reader 2, respectively. The rectum was best visualized in TRACE images and was scored 3.6 (SD: 1.3) and 3.3 SD: 1.0) by

reader 1 and reader 2. Lymph nodes in the mesorectum were also visible best in TRACE images, with mean scores of 3.2 (SD: 1.2) and 2.4 (SD: 0.8) for reader 1 and reader 2.

Figure 2 shows scatter plots of the individual scores of both readers. The quality of fat suppression in the mesorectum in TRACE was similar for both image sets (Fig 2a). No significant differences between the conventional and SMS diffusion weighted images were seen for both readers.

Interobserver agreement by weighted kappa-values for conventional DWI were calculated for overall image quality

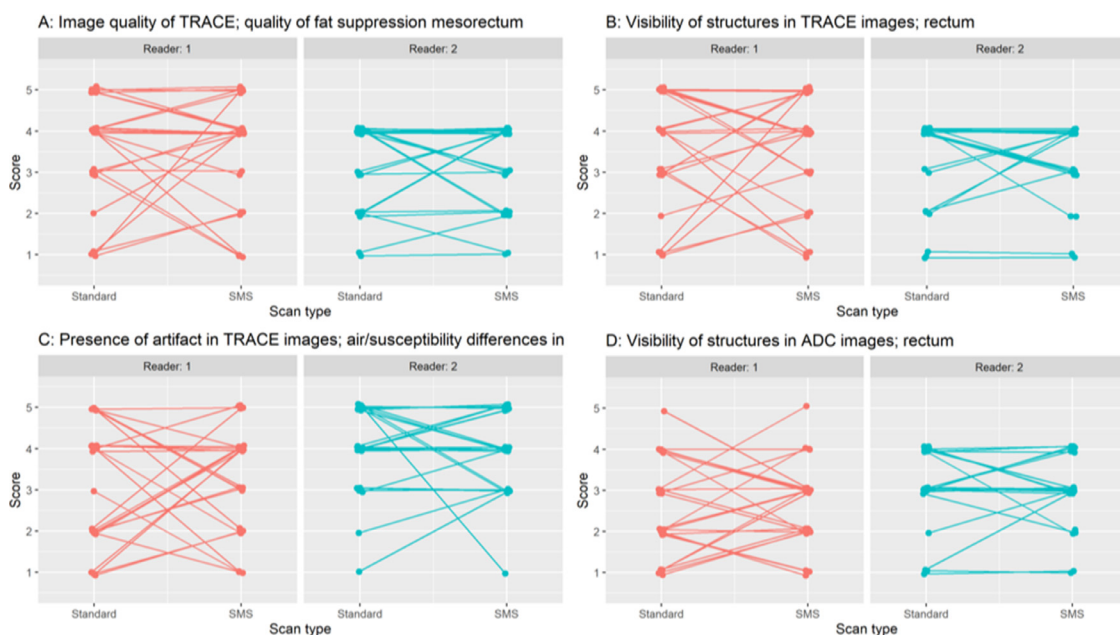


Figure 2. Scatter plots of individual scores of both readers. (Color version of figure is available online.)

of TRACE = 0.20 (CI; -0.16 to 0.42); calculated  $B$ -value (1000) = 0.08 (CI; -0.17 to 0.32) and ADC = 0.01 (CI -0.20 to 0.22). The weighted kappa-values for SMS DWI were calculated for overall image quality of TRACE = 0.22 (CI -0.11 to 0.57); calculated  $B$ -value (1000) = 0.30 (CI 0.04 to 0.56) and ADC = 0.12 (CI -0.02 to 0.26).

Mean scores of all variables scored by both readers can be found in Supplementary Table 1.

## DISCUSSION

In this study, we investigated the image quality of simultaneous multislice diffusion-weighted imaging of the rectum. We found that this technique is an effective approach to reduce acquisition time, while maintaining a similar image quality as compared to an optimized conventional reference DWI sequence.

Image quality in this work was assessed by two radiologists within a clinical setting. Defining an objective measure for SNR as a quantitative measure is not as easy as it seems, especially when multiple coils are used to receive the MR signal. MR signal addition of multiple coil elements depends on the local sensitivity of the coils at the location of interest. Relating MR signal to the noise level in air is problematic, as there is no signal (and with that no coil sensitivity estimate) but noise,  $g$ -factor noise and artefacts from motion present, so the coil addition in air is very different from MR signal addition at a particular location within the body. With artefacts from motion causing variation in noise from one measurement to the other, we decided not to quantify SNR.

An essential element in DWI of the pelvis is the suppression of lipid signals. Conventional se-EPI DWI uses spectrally selective fat excitation pulses with gradient crushers before every slice excitation to saturate lipid signals. The SMS-DWI sequence covers a larger FOV in the slice-dimension, over which the RF excitation field at 3T is often not homogeneous enough for satisfactory conventional fat saturation. Therefore, in this work, SPAIR was used to spectrally invert lipid signals with a broadband adiabatic inversion pulse, and excite the signals of interest at the moment lipid signals transit through zero magnetization in the  $z$ -direction. Compared to normal fat saturation, SPAIR needs additional time for the inversion and partial relaxation of lipid signals, and deposits more RF energy in the tissue with the adiabatic inversion pulse. However, with SMS-acceleration this time is available, and the reduced RF power deposition of simultaneous excitation and refocusing of slices compensates in part the additional power demand of the inversion pulse.

Our results are in line with previous studies describing the feasibility of SMS-DWI in other organs, showing similar or even higher image quality compared to conventional DWI protocol (11-13) in less acquisition time. In addition, visualization of essential structures, such as the rectum or lymph nodes was good to very-good in TRACE. These are encouraging results, demonstrating its potential application in general routine. With the ongoing trend towards more organ

preserving treatment of rectal cancer, a substantial increase in MRI imaging is to be expected (19-21). Thus, time efficient protocols are crucial considering the increasing importance of DWI in the management of a watch and wait strategy. Using the SMS-DWI sequence at a single table position, only one magnetic field homogeneity adjustment (shimming) and coil receive profile adjustment is necessary, which saves additional time compared to the conventional method, in which the patient table moves between two stations and two of both these adjustments are needed. The total acquisition time of a DWI sequence can be reduced with almost 50% if the conventional two-stage protocol is replaced with the single-stage SMS-DWI protocol.

Our results align with the work by Park et al (15) in patients with rectal cancer. They showed similar image quality between conventional DWI and SMS-DWI sequences with an acceleration factor of 2. Image quality was deteriorated significantly in most of the image quality parameters when using an acceleration factor of 3. Contrary to their work, we did not use endorectal filling, and used optimized conventional DWI with spectral fat saturation allowing the shortest measurement times for this method.

There are some limitations in our study that needs to be addressed. Quite some variability was present between the two readers who scored the images, both in average scores between the readers, as well as in scores of the two methods within a reader. Conventional DWI showed mostly a slight interobserver agreement for overall image quality, while the SMS DWI showed a fair agreement between the readers. This can be explained by the subjective Likert scoring methodology, in which reader 2 can be considered more critical, and perhaps more experienced in reading rectal MRI than reader 1. However, we do not believe this affects the conclusions presented in this paper, since we compared scores of the conventional versus the SMS-protocol per individual reader. The subjective scores on image quality and the variability per reviewer is in line with work from Obele et al, which described the image quality of SMS-DWI technique of the liver (13). They also reported a poor to moderate interobserver agreement from the results of the subjective image quality analysis, and used a comparable scoring protocol (1-5: non-diagnostic - excellent). Furthermore, no diagnostic criteria, such as visualization of a tumor and correlation with histopathological results were part of this study.

In conclusion, optimized SMS-DWI compared to conventional DWI in imaging of the rectum showed similar quality while a significant acquisition time reduction was achieved. We can suggest using the SMS protocol as standard of care in DWI of the rectum.

## ACKNOWLEDGMENT

We would like to thank SIEMENS Healthineers for providing the SMS-DWI protocol used in this study.

## REFERENCES

1. Beets-Tan RGH. Magnetic resonance imaging for clinical management of rectal cancer: updated recommendations from the 2016 European Society of Gastrointestinal and Abdominal Radiology (ESGAR) consensus meeting. *Eur Radiol* 2018; 28(4):1465–1475.
2. Rao SX. The value of diffusion-weighted imaging in combination with T2-weighted imaging for rectal cancer detection. *Eur J Radiol* 2008; 65(2):299–303.
3. Foti PV. Locally advanced rectal cancer: qualitative and quantitative evaluation of diffusion-weighted MR imaging in the response assessment after neoadjuvant chemo-radiotherapy. *Eur J Radiol Open* 2016; 3:145–152.
4. Song I. Value of diffusion-weighted imaging in the detection of viable tumour after neoadjuvant chemoradiation therapy in patients with locally advanced rectal cancer: comparison with T2 weighted and PET/CT imaging. *Br J Radiol* 2012; 85:577–586. 1013.
5. Stijns RCH. Advances in organ preserving strategies in rectal cancer patients. *Eur J Surg Oncol* 2018; 44(2):209–219.
6. Beddy D. A simplified tumor regression grade correlates with survival in locally advanced rectal carcinoma treated with neoadjuvant chemoradiotherapy. *Ann Surg Oncol* 2008; 15(12):3471–3477.
7. Smith JD. Nonoperative management of rectal cancer with complete clinical response after neoadjuvant therapy. *Ann Surg* 2012; 256(6):965–972.
8. Martin ST, Heneghan HM, Winter DC. Systematic review and meta-analysis of outcomes following pathological complete response to neoadjuvant chemoradiotherapy for rectal cancer. *Br J Surg* 2012; 99(7):918–928.
9. Beets GL. A new paradigm for rectal cancer: organ preservation: introducing the International Watch & Wait Database (IWW). *Eur J Surg Oncol* 2015; 41(12):1562–1564.
10. Larkman DJ. Use of multicoil arrays for separation of signal from multiple slices simultaneously excited. *J Magn Reson Imaging* 2001; 13(2):313–317.
11. Weiss J. Feasibility of accelerated simultaneous multislice diffusion-weighted MRI of the prostate. *J Magn Reson Imaging* 2017; 46(5):1507–1515.
12. Kenkel D. Simultaneous multislice diffusion-weighted imaging of the kidney: a systematic analysis of image quality. *Invest Radiol* 2017; 52(3):163–169.
13. Obele CC. simultaneous multislice accelerated free-breathing diffusion-weighted imaging of the liver at 3T. *Abdom Imaging* 2015; 40(7):2323–2330.
14. Taron J. Scan time reduction in diffusion-weighted imaging of the pancreas using a simultaneous multislice technique with different acceleration factors: how fast can we go? *Eur Radiol* 2018; 28(4):1504–1511.
15. Park JH. Feasibility of simultaneous multislice acceleration technique in diffusion-weighted magnetic resonance imaging of the rectum. *Korean J Radiol* 2020; 21(1):77–87.
16. Stijns RC. The influence of endorectal filling on rectal cancer staging with MRI. *Br J Radiol* 2018; 91:20180205. 1089.
17. Deurenberg P, Deurenberg-Yap M, Guricci S. Asians are different from Caucasians and from each other in their body mass index/body fat per cent relationship. *Obes Rev* 2002; 3(3):141–146.
18. Landis JR, Koch GG. The measurement of observer agreement for categorical data. *Biometrics* 1977; 33(1):159–174.
19. van der Valk MJM. Long-term outcomes of clinical complete responders after neoadjuvant treatment for rectal cancer in the International Watch & Wait Database (IWW): an international multicentre registry study. *Lancet* 2018; 391(10139):2537–2545.
20. Bernier L. Watch-and-wait as a therapeutic strategy in rectal cancer. *Curr Colorectal Cancer Rep* 2018; 14(2):37–55.
21. Lopez-Campos F. Watch and wait approach in rectal cancer: current controversies and future directions. *World J Gastroenterol* 2020; 26(29):4218–4239.

## SUPPLEMENTARY MATERIALS

Supplementary material associated with this article can be found in the online version at doi:10.1016/j.acra.2022.02.005.